J. Min. Metall. Sect. B-Metall. 51 (1) B (2015) 67 - 72

Journal of Mining and Metallurgy,
Section B: Metallurgy

DIRECTIONAL SOLIDIFICATION OF Zn–Al–Cu EUTECTIC ALLOY BY THE VERTICAL BRIDGMAN METHOD

U. Büyük [a,*], S. Engin [b], N. Maraşlı [c]

[a] Department of Science Education, Faculty of Education, Erciyes University, Kayseri, Turkey
[b] Department of Energy Systems Engineering, Faculty of Technology,
Dumlupınar University, Kütahya, Turkey
[c] Department of Metallurgical and Materials Engineering, Faculty of Chemical and Metallurgical
Engineering, Yıldız Technical University, İstanbul, Turkey

(Received 04 March 2014; accepted 21 November 2014)

Abstract

In the present work, the effect of growth rate and temperature gradient on microstructure and mechanical properties of Zn–7wt.%Al–4wt.%Cu eutectic alloy has been investigated. Alloys prepared under steady-state conditions by vacuumed hot filing furnace. Then, the alloys were directionally solidified upward with different growth rates (V=11.62–230.77 μm/s) at a constant temperature gradient (G=7.17 K/mm) and with different temperature gradients (G=7.17–11.04 K/mm) at a constant growth rate (V=11.62 μm/s) by a Bridgman furnace. The microstructures were observed to be lamellae of Zn, Al and broken lamellae $CuZn_4$ phases from quenched samples. The values of eutectic spacing, microhardness and ultimate tensile strength of alloys were measured. The dependency of the microstructure and mechanical properties on growth rate and temperature gradient were investigated using regression analysis.

Keywords: Solidification; Microstructure; Eutectic spacing; Hardness test; Tensile test

1. Introduction

Melting and solidification are between the non-crystallographic and crystallographic states of a metal or alloy. An understanding of the mechanism of solidification is important in the control of the mechanical and electrical properties of cast metals [1].

Unidirectional solidification of eutectic alloys has received considerable attention in the past few years because the alignment of the rods, lamellae, fibers or plates in some of these eutectics produces attractive physical or mechanical properties. Most of the works have been done on binary alloys at eutectic and near eutectic compositions, and only some works have been initiated recently in the area of ternary and quaternary eutectic alloys.

Zn, Al and Cu alloys have a number of advantages such as low cost, excellent castability, high resistance to wear, abrasion and good emergency [2–7]. The zinc-based alloys are in general based on Zn–Al eutectic, eutectoid or monotectoid compositions. Copper has been used as the main alloying element to improve the mechanical and tribological properties of Zn–Al alloys [8, 9]. The effect of growth rate on the hardness properties of Zn–5wt.%Al eutectic and Zn–0.7wt.%Cu hypo-peritectic alloys had been investigated systematically by the authors of this paper [10–11]. It has been shown that, as the hardness of the alloys increase, the eutectic spacing decreases with increasing growth rate [10–11]. But the hardness and strength of binary Zn–Al eutectic alloys are not adequate for most of the engineering applications. However, the effect of copper content on the microstructure and mechanical properties of eutectic Zn–Al based alloys, which are successfully used in engineering applications, has not been well understood.

The purpose of the present work is to investigate the microstructure morphology and mechanical properties of Zn–7wt.%Al–4wt.%Cu eutectic alloy under different solidification conditions. For this purpose, the dependency of eutectic spacing (λ_{Zn-Al} and $\lambda_{CuZn_4-CuZn_4}$), Vickers microhardness (HV) and ultimate tensile strength (σ_{uts}) on the solidification processing parameters (growth rate, V and temperature gradient, G) of directionally solidified Zn–7wt.%Al–4wt.%Cu eutectic alloy were investigated.

2. Experimental Procedure

In the present work, the experimental procedure

* *Corresponding author: buyuk@erciyes.edu.tr*

DOI:10.2298/JMMB140304007B

consists of alloy preparation, directional solidification, microstructure observation and identification of phases, measurements of eutectic spacing, microhardness and ultimate tensile strength of the directional solidified Zn–7wt.%Al–4wt.%Cu eutectic alloy.

2.1 Alloy preparation and directional solidification

The composition of the Zn–Al–Cu ternary eutectic alloy was chosen to be Zn–7wt.%Al–4wt.%Cu. Zn–Al–Cu alloy was prepared under the vacuum using pure zinc, aluminum and copper (>99.99%) and poured into 30 graphite crucibles (200×4ID×6.35OD mm) held in a hot filling furnace at the 50 ºC above the melting point of the alloy. The melted alloy was directionally solidified and then, each sample was positioned in a Bridgman furnace. The samples were solidified with different growth rates (V=11.62–230.77 μm/s) at a constant temperature gradient (G=7.17 K/mm) and with different temperature gradients (G=7.17–11.04 K/mm) at a constant growth rate (V=11.62 μm/s) using synchronous motors having various speed. The block diagram of the experimental setup and details of the solidification furnace is shown in Fig. 1.

The quenched sample was removed from the graphite crucible and cut into lengths typically 8 mm. They are mounted with epoxy–resin, polished and ultrasonically cleaned. Then, the samples were etched with 5 ml hydrofluoric acid in 95 ml water for 15 seconds.

2.2 Microstructure observation and identification of phases

The microstructures of samples were analyzed by LEO Scanning Electron Microscope (SEM) and Olympus BX51 Optical Microscope. Different growth rates and temperature gradient were applied to explore the possible formation of phases in the eutectic Zn–Al–Cu alloy. The typical images of growth morphologies for directional solidified Zn–7wt.%Al–4wt.%Cu eutectic alloy are shown in Fig. 2. The sample exhibits a full eutectic microstructure consisting of regular lamellae of Zn, Al and broken (quasi-regular) lamellae $CuZn_4$ phase.

According to the phase diagram of Zn–Al–Cu ternary alloy [12], eutectic reaction at eutectic temperature: $L \rightarrow \eta\text{–}Zn + \alpha\text{–}Al + \varepsilon\text{–}CuZn_4$. The quantitative chemical composition analysis of regular lamella of Zn, Al and broken lamellae $CuZn_4$ phases were carried out by using energy dispersive X–ray analysis (EDX) and given in Fig. 2. According to phase diagram and EDX results light grey, dark grey and white phases were identified as η–Zn, α–Al and ε–$CuZn_4$, respectively.

The Zn and Al phase forms as regular lamellae during unidirectional solidification of Zn–Al eutectic [10]. Similarly, both Zn and Al phases form as regular lamellae, but $CuZn_4$ phases form as broken quasi-regular lamellae. This structure was observed in all of different solidification parameters and the any primary dendrites were not also observed at high solidification velocities. It can be seen from Fig. 2 that the $CuZn_4$ phase is generally contained within the

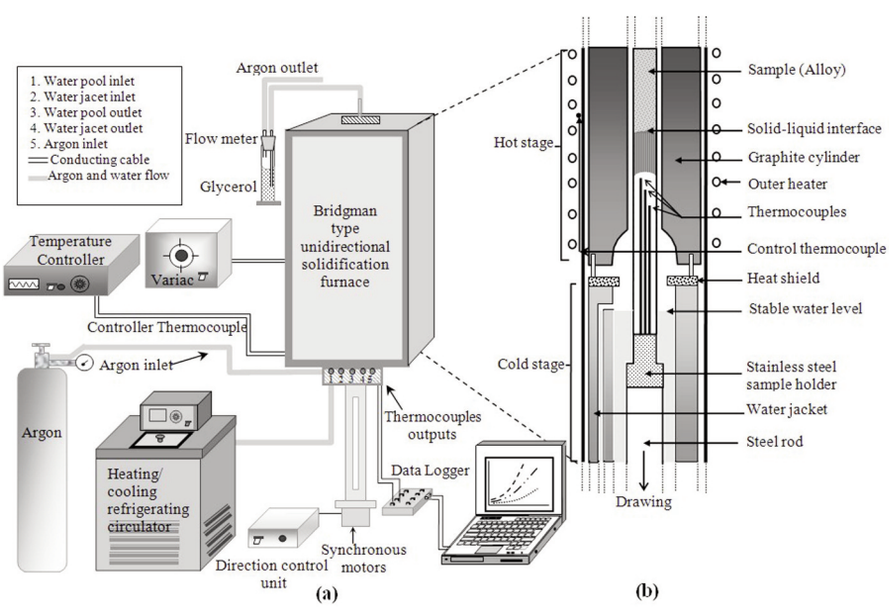

Figure 1. *(a) Block diagram of the experimental setup, (b) The details of the Bridgman type directional solidification furnace.*

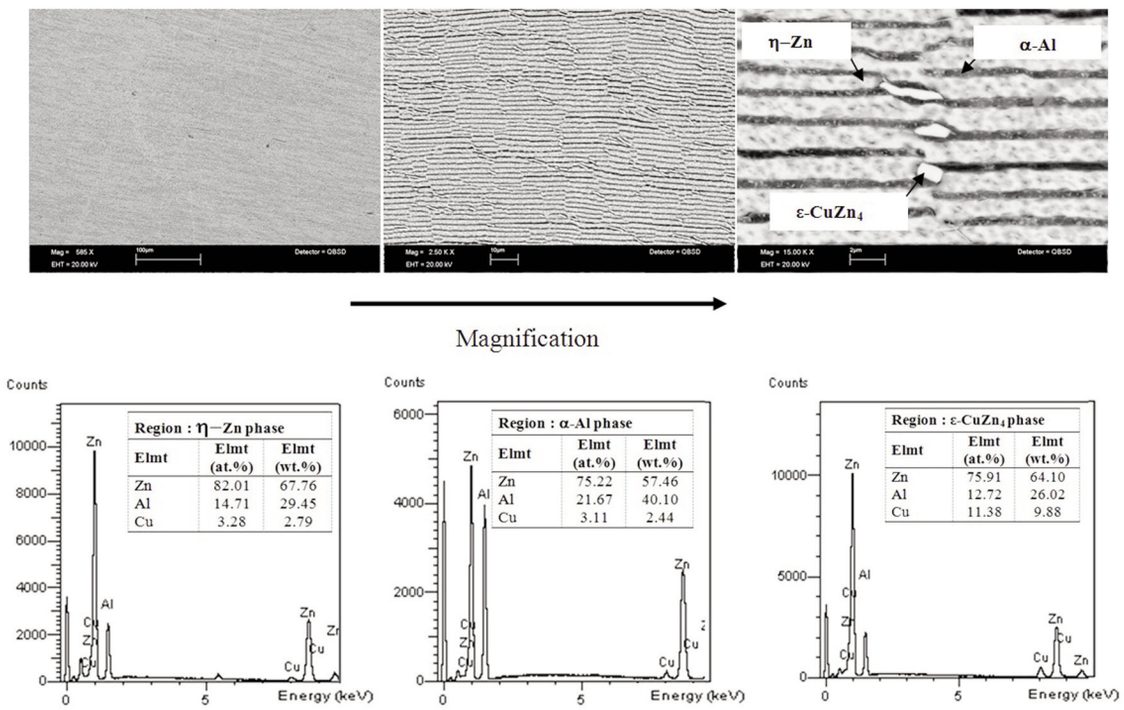

Figure 2. *Typical SEM images with different magnifications and the chemical composition analysis of directional solidified Zn–7Al–4Cu eutectic alloy (V= 11.62 µm/s and G= 11.05 K/mm).*

Al-rich (α) phase. A possible reason for the growth of the $CuZn_4$ phase preferentially in the Al-rich (α) phase probably has relatively low interfacial free energy of Zn. The interface within all three phases was planar, during the unidirectional solidification process.

2.3. The measurement of solidification parameters and eutectic spacing

The growth rates were recorded by a data–logger via computer during the growth. The temperature in the specimen was measured with three thermocouples insulated (K–type, 0.25 mm in diameter). The value of growth rate ($V=\Delta X/\Delta t$) in the solid phase and temperature gradient ($G=\Delta T/\Delta X$) for each sample was determined. Details of the measurements of ΔT, ΔX and Δt are given in Refs. [13–14].

The measurements of eutectic spacing were made from the photographs of microstructures with a linear intercept method [15]. The measured values of the eutectic spacing (eutectic spacing between zinc and aluminum phases, λ_{Zn-Al}, and eutectic spacing between $CuZn_4$ and $CuZn_4$ phases, $\lambda_{CuZn_4-CuZn_4}$) in the Zn–Al–Cu alloy are given in Fig. 3.

2.4. The measurement of mechanical properties

The mechanical properties of any solidified materials are usually determined with hardness test, tensile strength test, etc. The microstructure formation

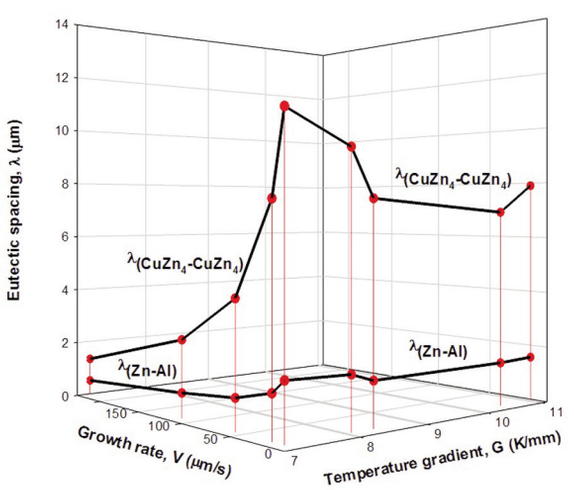

Figure 3. *Variations of eutectic spacing as a function of growth rate and temperature gradient.*

of the directionally solidified alloys is crucial for mechanical properties. Therefore, the microhardness and ultimate tensile strength values were measured by using a microhardness and tensile test device.

One of the aims of this work was to learn the relationships between the growth rate/ temperature gradient and microhardness for directional solidified Zn–Al–Cu eutectic alloy. The Vickers hardness (HV) is the ratio of a load applied to the indenter to the

surface area of the indentation. Measurements were made with a ***Future–Tech FM–700*** model hardness measuring test device using a 500 g load, and a dwell time of 10 s gives a typical indentation depth of about 40–60 μm. Microhardness values are averages of at least 20 measurements on the transverse sections. Variations of HV with the V and G the Zn–Al–Cu eutectic alloys are plotted in Fig. 4.

Another aim of this work was to experimentally investigate the effect of the growth rate/ temperature gradient on the ultimate tensile strength of the directional solidified Zn–Al–Cu alloy. The measurements of ultimate tensile strength were made at room temperature at a strain rate of 10^{-3} s^{-1} with a ***Shimadzu Universal Testing Instrument*** (Type AG–10KNG). In order to avoid damaging the sample surface, two seals were stuck on the sample instead of the traditional clip gauge. The round rod tensile samples with the diameter of 4 mm and gauge lengths of 100 mm were prepared from directional solidified rod samples with different solidification parameters. The tensile axis were chosen in parallel with the growth direction of the sample, and the tests were repeated two times. Variations of ultimate tensile strength with the growth rate and temperature gradient for the Zn–Al–Cu eutectic alloys are plotted in Fig. 5.

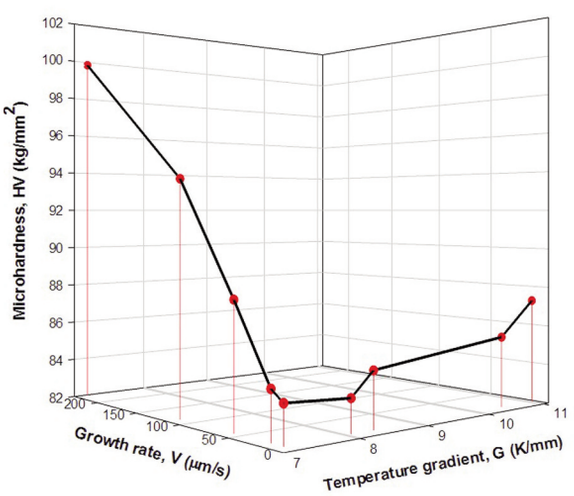

Figure 4. *Variation of microhardness as a function of growth rate and temperature gradient.*

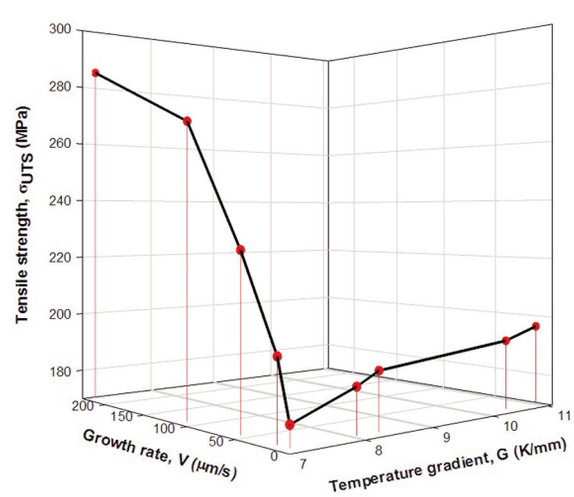

Figure 5. *Variation of ultimate tensile strength as a function of growth rate and temperature gradient.*

3. Results and Discussion

3.1. The effect of solidification parameters on the eutectic spacing

The eutectic spacing of Zn–Al–Cu alloys for different growth rates and temperature gradients were measured and given in Fig. 3. As expected, as the growth rate and temperature gradient increase, the eutectic spacing decreases. When the growth rate of samples increases from 11.62 to 230.77 μm/s, the average eutectic spacing for λ_{Zn-Al} (spacing of between Zn and Al phases) and $\lambda_{CuZn_4-CuZn_4}$ (spacing of between $CuZn_4$ and $CuZn_4$ phases) decrease from 1.93 μm to 0.52 μm and from 10.10 μm to 1.34 μm, respectively. As can be seen from Fig. 3, the V is more effective than the G on the λ.

The variation of λ versus V is essentially linear on the logarithmic scale. The relationships between the eutectic spacing and growth rates were determined as $\lambda_{Zn-Al} = 5.49(V)^{-0.42}$ and $\lambda_{CuZn_4-CuZn_4} = 35.48(V)^{-0.56}$ by using linear regression analysis. The values of the exponent relating to the growth rates (0.42 for regular lamellae of Zn–Al in the ternary Zn–Al–Cu eutectic alloy) obtained in this work are in agreement with the values of 0.53 for regular lamellae of Zn–Al in the binary Zn–Al eutectic alloy ($\lambda_{Zn-Al} = 9.21(V)^{-0.53}$) [10]. Similarly, the values of the exponent relating to the growth rates obtained in this work are in good agreement with the values of 0.46–053 obtained by various works [16-22].

The relationships between the eutectic spacing and temperature gradient were determined as $\lambda_{Zn-Al} = 4.57(G)^{-0.46}$ and $\lambda_{CuZn_4-CuZn_4} = 32.35(G)^{-0.62}$ by using linear regression analysis. The values of the exponent relating to the temperature gradient obtained 0.42 is in good agreement with the value of 0.40–0.53 obtained by various works [20-24]. But, 0.62 which values of the exponent relating to the $CuZn_4$ phase are higher than similar work [20-24]. A possible reason for the this high value can be quasi regular growth of $CuZn_4$ phase.

3.1. The effect of solidification parameters on mechanical properties

The microhardness and ultimate tensile strength

for different solidification parameters were measured and given in Figs. 4 and 5. It can be seen from Figs. 4 and 5 that an increase in growth rates and temperature gradients leads to an increase in the HV and σ_{UTS}.

For Zn–7wt.%Al–4wt.%Cu eutectic alloy which is a semi-hard materials; as the growth rate increases from 11.62 to 230.77 µm/s, the microhardness increases from 84.34 to 99.84 kg/mm^2. It can be observed that a decrease in the λ values leads to an increase in the HV values.

The results obtained in the present work for Zn–Al–Cu eutectic alloy was compared with Zn–5wt.%Al eutectic alloy [10] and Zn–0.7wt.%Cu hypo–peritectic alloy [11], and given in Fig. 6. The values of HV (from 84.34 to 99.84 kg/mm^2) for different growth rates for directionally solidified Zn–Al–Cu eutectic alloy obtained in the present work are higher than the values of HV for the Zn–5wt.%Al (from 55.98 to 88.91 kg/mm^2) [10] and Zn–0.7wt.%Cu alloy (from 53.10 to 66.3 kg/mm^2) [11], solidified under similar conditions.

The relationship between the HV and V was determined to be $HV = 67.60(V)^{0.07}$ for Zn–Al–Cu eutectic alloy by linear regression analysis. This exponent value agrees with the exponent values of V (0.07–0.11) obtained by various researchers [25–30] for different binary and ternary eutectic alloy systems.

The exponent values of HV relating to the growth rate for directionally solidified Zn–Al–Cu eutectic alloy obtained in the present work are slightly lower than the exponent values of HV relating to V for the Zn–5wt.%Al eutectic alloy ($HV = 115.65(V)^{0.13}$) [10]. Moreover, this exponent value is same with Zn–0.7wt.%Cu hypo peritectic alloy ($HV = 70.15(V)^{0.07}$) [11].

On the other hands, the relationship between the HV and G was determined to be $HV = 70.79(G)^{0.08}$ for Zn–Al–Cu eutectic alloy by linear regression analysis. The exponent values of alloy obtained in the present work are slightly lower than the exponent values for the Zn–0.7wt.%Cu hypo peritectic alloy ($HV = 46.03(G)^{0.14}$) [11] in a good agreement with the exponent values relating to the G (0.11–0.19) obtained in previous experimental works [31–32] for different binary and ternary eutectic alloy systems.

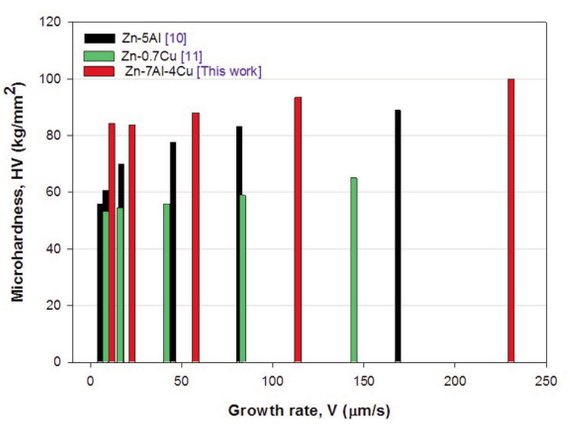

Figure 6. *A comparison of microhardness values of Zn–7Al–4Cu alloys with Zn–5Al and Zn–0.7Cu alloys for different growth rates alloy.*

Fig. 5 shows the variation of the ultimate tensile strength (stress) values with the growth rate and temperature gradient. The relationship between σ_{UTS} and V was found to be $\sigma_{UTS} = 123.02(V)^{0.16}$ and between σ_{UTS} and G was found to be $\sigma_{UTS} = 114.81(G)^{0.22}$ by linear regression analysis, and also it can be seen that the values of the ultimate tensile strength increase with increasing growth rate and temperature gradient. It is found that if the growth rate increases from 11.62 µm/s to 230.77 µm/s, the ultimate tensile strength increases from 176.55 to 285.43 MPa. Besides the temperature gradient increases from 7.17 µm/s to 11.04 µm/s, the ultimate tensile strength increases from 176.55 to 196.55 MPa. The growth rate is more effective than the temperature gradient on the ultimate tensile strength.

The exponent values of σ_{UTS} relating to the V and G for directionally solidified Zn–Al–Cu eutectic alloy obtained in the present work are lower than the values for the Al–11.1wt%Si–4.2wt% eutectic alloy ($\sigma_{UTS} = 37.15(V)^{0.19}$, $\sigma_{UTS} = 35.48(G)^{0.26}$) [33].

4. Conclusions

In the present work, Zn–7wt.%Al–4wt.%Cu eutectic alloy was solidified unidirectionally and the microstructures were observed to be both Zn and Al phases form as regular lamellae during solidification of Zn–7wt.%Al–4wt.%Cu eutectic, but $CuZn_4$ phases form as broken quasi–regular lamellae. This structure is observed in all of different solidification parameters and any primary dendrites were not observed at high growth rates. The interface within all three phases was planar, during the unidirectional solidification process.

The eutectic spacing, microhardness and ultimate tensile strength values for directional solidified Zn–7wt.%Al–4wt.%Cu eutectic alloy have been measured. The eutectic spacing values, λ_{Zn-Al} for the Zn–7wt.%Al–4wt.%Cu eutectic alloy were found to be higher than the Zn–5wt.%Al eutectics. The microhardness values for the Zn–7wt.%Al–4wt.%Cu eutectic alloy were found to be higher than the Zn–5wt.%Al eutectic and Zn–0.7wt.%Cu hypo peritectic alloy.

The relationships among eutectic spacing, microhardness, ultimate tensile strength and growth rates/temperature gradient were obtained by regression analysis as, $\lambda_{Zn-Al} = 5.49(V)^{-0.42}$, $\lambda_{CuZn_4-CuZn_4} = 35.48(V)^{-0.56}$, $\lambda_{Zn-Al} = 4.57(G)^{-0.46}$, $\lambda_{CuZn_4-CuZn_4} = 32.35(G)^{-0.62}$, $HV = 67.60(V)^{0.07}$, $HV = 70.79(G)^{0.08}$;

$\sigma_{UTS} = 123.02(V)^{0.16}$ and $\sigma_{UTS} = 114.81(G)^{0.22}$, respectively.

References

[1] D.A. Porter, K.E. Easterling, Phase transformations in metals and alloys, Second Edition, CRC Press, 1992, p.185.

[2] T. Savaşkan, G. Pürçek and S. Murphy, Wear, 252 (2002) 693-703.

[3] G. Pürçek, T. Savaşkan, T. Küçükömeroğlu and S. Murphy, Wear, 252 (2002) 894-901.

[4] I.A. Figueroa, O. Novelo-Peralta, M.A. Suárez, G.A. Lara-Rodríguez, J. Min. Metall. Sect. B-Metall. 49 (3) B (2013) 293–297.

[5] L. Čelko, L. Klakurková, B. Smetana, K. Slámečka, M. Žaludová, D. Hui, J. Švejcar, J. Min. Metall. Sect. B-Metall. 50 (1) B (2014) 31–36.

[6] L.M. Zhang, M.L. Chen, C.K. Yan, J. Mater. Sci. Lett., 17 (1998) 1903-1905.

[7] B.K. Prasad, A.K. Patwardhan, A.H. Yegneswaran, Metall. Mater. Trans., 27A (1996) 3513-3523.

[8] B.K. Prasad, Mater. Charact., 44 (2000) 301-308.

[9] B.K. Prasad, Metallkd Z., 88 (1997) 929-933.

[10] S. Engin, U. Böyük, H. Kaya, N. Maraşlı, Int. J. Min. Met. Mater., 14(2) (2011) 659-664.

[11] H. Kaya, U. Böyük, S. Engin, E. Çadırlı, N. Maraşlı, J. Electron. Mater., 39(3) (2010) 303-311.

[12] H. Liang, Y.A. Chang, J. Phase Equilibria., 19(1) (1998) 25-37.

[13] E. Çadırlı, M. Gündüz, J. Mater. Proceess. Tech., 97 (2000) 74-81.

[14] M. Gündüz, H. Kaya, E. Çadırlı, A. Özmen, Mat. Sci. Eng. A, 369 (2004) 215-229.

[15] A. Ourdjini, J. Liu, R. Elliott, Mater. Sci. Tech–Lond., 10 (1994) 312-318.

[16] U. Böyük, N. Maraşlı. J. Alloy. Compd., 485 (2009) 264-269.

[17] J. De Wilde, L. Froyen, S. Rex, Scripta Mater., 51 (2004) 533-538.

[18] E. Çadırlı, U. Böyük, H. Kaya, N. Maraşlı, K. Keşlioğlu, S. Akbulut, Y. Ocak, J. Alloy Compd., 470 (2009) 150-156.

[19] V.T. Witusiewicz, U. Hecht, S. Rex, M. Apel, Acta Mater., 53 (2005) 3663-3669.

[20] U. Böyük, N. Maraşlı, H. Kaya, E. Çadırlı, K. Keşlioğlu, Appl. Phys. A–Mater., 95 (2009) 923-932.

[21] U. Böyük, S. Engin, H. Kaya, N. Maraşlı, Mater. Charact., 61 (2010) 1260-1267.

[22] U. Böyük, S. Engin, N. Maraşlı, Mater. Charact., 62(9) (2011) 844-851.

[23] H. Kaya, U. Böyük, E. Çadırlı, Y. Ocak, S. Akbulut, K. Keslioglu, N. Maraşlı, Met. Mater. Int., 14(5) (2008) 575-582.

[24] N. Maraşlı, U. Böyük, Mater. Chem. Phys., 119 (2010) 442-448.

[25] F. Vnuk, M. Sahoo, R. Van De Merwe, R.W. Smith, J. Mater. Sci. 14 (1979) 975-982.

[26] F. Vnuk, M. Sahoo, D. Baragor, R.W. Smith, J. Mater. Sci., 15 (1980) 2573-2583.

[27] A.I. Telli, S.E. Kısakürek, Mat. Sci. and Tech., 4 (1988) 153-156.

[28] E. Çadırlı, U. Böyük, H. Kaya, N. Maraşlı, K. Keşlioğlu, S. Akbulut, Y. Ocak, J. Alloy Compd., 470 (2009) 150-156.

[29] U. Böyük, N. Maraşlı, J. Alloy Compd., 485 (2009) 264-269.

[30] E. Çadırlı, U. Böyük, S. Engin, H. Kaya, N. Maraşlı, Kovove Mater., 47 (2009) 381-387

[31] H. Kaya, E. Çadırlı, U. Böyük, N. Maraşlı, App. Surf. Sci., 255 (2008) 3071-3078.

[32] U. Böyük, N. Maraşlı, Mater. Chem. Phys., 119 (2010) 442-448.

[33] U. Böyük, Met. Mater. Int., 18(6) (2012) 933-938.